Contrast-Enhanced MRI with Gadodiamide Injection in Rat Disease Models

Kazutaka YAMADA[1, 2, 3]*, Kazuro MIYAHARA[1], Hiroshi SATO[2], Wakako NAKAYAMA[2], Motoyoshi SATO[1], Tsuneo HIROSE[1], Hirotoshi KATO[3], Hiroo IKEHIRA[3], Yukio TATENO[3], Hiroshi SUGIHARA[2], and Kazuhisa FURUHAMA[2]

[1]*Department of Veterinary Clinical Radiology, Obihiro University of Agriculture and Veterinary Medicine, Obihiro 080,* [2]*Daiichi Pharmaceutical Co., Ltd., Tokyo 134, and* [3]*National Institute of Radiological Sciences, Chiba 263, Japan*

(Received 11 May 1995/Accepted 25 October 1995)

ABSTRACT. The present study was designed to confirm the usefulness of contrast-enhanced magnetic resonance imaging (MRI) in diagnosing strokes of stroke-prone spontaneously hypertensive rats (SHRSP) and middle cerebral artery (MCA) occlusion, hepatocellular carcinoma and hydronephrosis of each experimental rat model. Male Sprague-Dawley rats (250–500 g), male SHRSP (ca. 250 g) and male F344 rats (ca. 300 g) were used for the investigation. Gadodiamide injection (Omniscan, Daiichi Pharmaceutical Co., Ltd. and Nycomed AS, Norway) was administered intravenously as the contrast agent at a dose of 0.1 mmol/kg except in hydronephrosis, where a dose of 0.05 mmol/kg was used. Magnetic resonance (MR) images were obtained with a 1.5 T or a 2.0 T magnetic field strength MRI unit. The signal intensity of the stroke lesions was increased after administration of gadodiamide injection in SHRSP and MCA-occluded rats. Hepatocellular carcinoma was undetectable without the use of the contrast agent, but the signal intensity of the tumor increased after administration of the gadodiamide injection, allowing the lesions to be detected. The signal intensity of the renal medulla increased in the non-ligated kidney, but not in the hydronephrotic kidney. The information given by the post-contrast images were superior to those obtained from the pre-contrast images in all the models. Contrast effects in SHRSP and MCA-occluded rats were related to differences in capillary permeability, those in rats with hepatocellular carcinoma depended on differences in vascularity, and those in hydronephrotic rats depended on blood flow and permeability. — KEY WORDS: gadodiamide injection, MRI, rat.

J. Vet. Med. Sci. 58(4): 291–295, 1996

Recently, magnetic resonance imaging (MRI) has been widely used in the veterinary field. Some studies have been performed using MRI units of high magnetic field strength (4.7–7.05 T) [10, 19], others with units of low magnetic field strength (0.2 T) [17, 36]. One of the characteristics of MRI is that it frequently allows the detection of small neoplastic lesions without the use of a contrast agent [20], although, limitations for performing complete diagnoses of the tissue damage such as brain stroke, liver tumor or hydronephrosis are still present. Meglumine gadopentetate, an ionic gadolinium derivative, has been widely used as a contrast agent in MRI. Gadodiamide injection (Omniscan, Daiichi Pharmaceutical Co., Ltd., and Nycomed AS, Norway) is a nonionic, paramagnetic gadolinium chelate newly developed as an MRI contrast agent whose safety has been demonstrated [14, 22, 31]. The characteristic of this agent is it's extracellular distribution and effectively enhances signal intensity in T1-weighted imaging [14, 22, 31]. There have, however, been few reports dealing with contrast-enhanced MRI in various spontaneous diseases or disease models of rats, related to the tissue damage described above. The purpose of the present study was to confirm the diagnostic potential of contrast-enhanced MRI using a MRI unit of medium magnetic field strength (1.5–2.0 T) to examine stroke-prone spontaneously hypertensive rats (SHRSP), and rats with experimental middle cerebral artery (MCA) occlusion, hepatocellular carcinoma and hydronephrosis.

* CORRESPONDENCE TO: YAMADA K., Department of Veterinary Clinical Radiology, Obihiro University of Agriculture and Veterinary Medicine, Inada-cho, Obihiro 080, Hokkaido, Japan.

MATERIALS AND METHODS

Animals: Male Sprague-Dawley (SD) rats, male Fischer 344 (F344) rats purchased from Charles River Japan, Inc. (Kanagawa, Japan) and male stroke-prone spontaneously hypertensive rats (SHRSP) kept at Daiichi Pharmaceutical Co., Ltd., were used in the investigation. These animals were housed in raised mesh-bottom cages in a ventilated room with a controlled temperature (23 ± 2°C) and relative humidity (55 ± 15%) under a 12-hr light/dark cycle. They were allowed free access to commercial laboratory chow (F-2: Funabashi Farm, Chiba, Japan) and tap water. Prior to the experiment, the animals were fasted for at least 18 hr. All animals were anesthetized with an intraperitoneal administration of chloral hydrate (40 mg/100 g). A 24-gauge indwelling needle was implanted into the tail vein, then the rats were placed inside the scan system in the prone position.

MRI units: Images were obtained with a 1.5 T Gyroscan S15 (Philips Medical Systems, Netherlands) or a 2.0 T RS-200 (Siemens-Asahi Medical Systems, Tokyo, Japan). Radio frequency pulses were at 64 MHz with the 1.5 T MRI unit, and at 85 MHz with the 2.0 T MRI unit. Each MRI unit incorporated a super-conductive magnet. A 4 cm diameter human temporomandibular joint coil for MCA [34, 37] and a 50 cm diameter human head coil for hydronephrosis were used as radio frequency coils in the 1.5 T magnetic field strength unit, and a 6 cm diameter

custom-made solenoid coil for SHRSP and hepatocellular carcinoma was employed in the 2.0 T unit. In this study, all images were T1-weighted because gadolinium shortens T1 relaxation time [20, 33].

Contrast agent: The gadodiamide injection was composed of gadolinium (III) diethylenetriaminepentaacetic acid bis-methylamide (GdDTPA-BMA) at a concentration of 500 mmol/*l* and the sodium calcium complex of the same ligand, known as caldiamide sodium (CaNaDTPA-BMA) at a concentration of 25 nmol/*l*. This contrast agent reduces T1 relaxation times and its relaxivity in water at 10 MHz and at 37°C is 4.6 $(mmol/L)^{-1}sec^{-1}$. Its viscosity is 2.8 cp at 20°C and 1.9 cp at 37°C [14, 22, 31]. In this study, the gadodiamide injection was administered intravenously at a dose of 0.1 mmol/kg or 0.05 mmol/kg for hydronephrosis. The displayed contrast was adjusted automatically in each scan, and the images had an effect on motion artifact, so the measured signal intensity was very unstable. The contrast effects were therefore evaluated visually [9, 16, 17, 19, 29, 30].

Animal models

SHRSP: Male SHRSP (ca. 250 g, n=2) showing periodic spasms were used at the age of 8 months.

MCA occlusion: Male SD rats (ca. 250 g, n=8) underwent an operation under microscopy to block the middle cerebral artery and were examined at 10 days post-operation [27].

Hepatocellular carcinoma: Male F344 rats (ca. 300 g, n=6) were administered drinking water containing 60 ppm diethylnitrosamine for 10 consecutive weeks to induce hepatocellular carcinoma, and were scanned 10 weeks after the commencement of treatment [32]. In this case, no respiratory gate was performed, so a short repetition time (100 msec) was selected to preclude respiratory motion artifacts [5, 12, 25].

Hydronephrosis: Male SD rats (ca. 500 g, n=6) were subjected to an operation to ligate the left ureter and were examined on the day after the operation.

Histological examination

After completion of the imaging protocol, all animals were subjected to euthanasia by exsanguination under chloral hydrate anesthesia, and the relevant diseased organs were inspected macroscopically. Tissue samples were fixed in 10% buffered formalin and embedded in paraffin wax. Thin sections of 4 μm thickness were prepared, stained with hematoxylin and eosin (H.E.) and examined histologically to evaluate the lesion.

RESULTS

SHRSP: In the two rats, similar MR images were obtained. In one rat (Fig. 1), lesions showed a wide low-signal-intensity area in the cortex and 2 low-signal-intensity areas in the thalamus in the pre-contrast images, and another lesion appeared as an enhanced spot between the 2 low-signal-intensity areas in post-contrast imaging. In the histological examination, focal thrombosis with hemorrhage, malacia and a few glial cells around the periphery of the thrombus were observed.

MCA occlusion: No lesion was seen in the pre-contrast images, but the stroke lesion was enhanced in the post-contrast images in all the rats examined (n=8) (Fig. 2). In

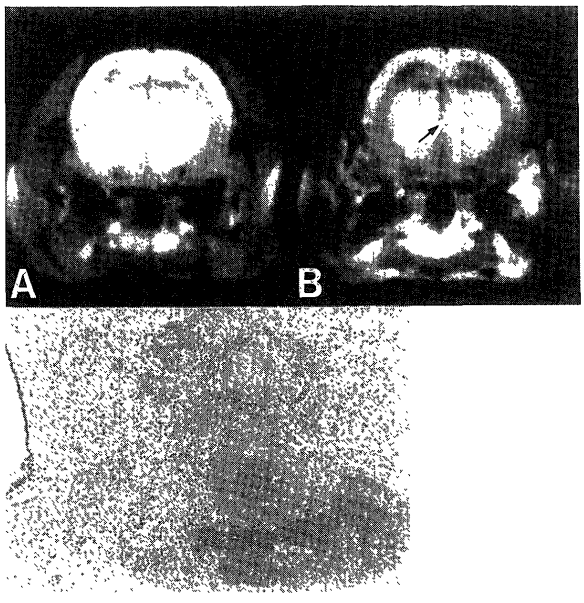

Fig. 1. Transverse T1-weighted image (Spin echo, TR/TE=500/30 msec) of a SHRSP. (A: Pre-contrast image. B: Post-contrast image. C: Photomicrograph, H.E. stain, × 100). In the pre-contrast image, lesions of a wide low-signal-intensity area in the cortex and 2 low-signal-intensity areas in the thalamus are shown. In the post-contrast image, another lesion (arrow) is enhanced between the 2 low-signal-intensity areas.

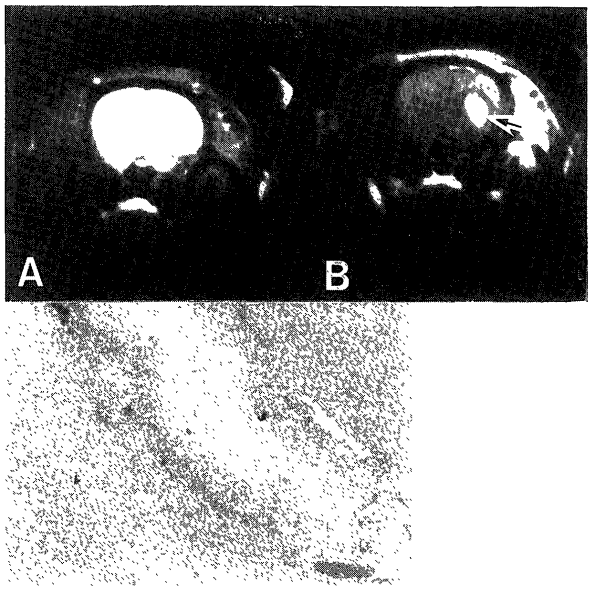

Fig. 2. Transverse T1-weighted image (Spin echo, TR/TE=200/30 msec) of MCA occlusion. (A: Pre-contrast image. B: Post-contrast image. C: Photomicrograph, H.E. stain, × 100). In the pre-contrast image, no lesion is seen, but in the post-contrast image, a stroke lesion is enhanced (arrow).

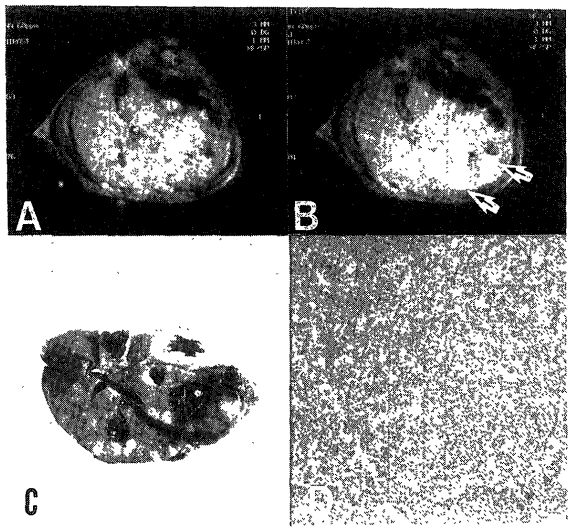

Fig. 3. Transverse T1-weighted image (Saturation recovery, TR/TE=100/10 msec) of hepatocellular carcinoma. (A: Pre-contrast image. B: Post-contrast image. C: Gross appearance. D: Photomicrograph, H.E. stain, × 200). In the pre-contrast image, the lesion could not be detected. Immediately after administration of gadodiamide injection, markedly enhanced areas (arrows) were seen in the liver.

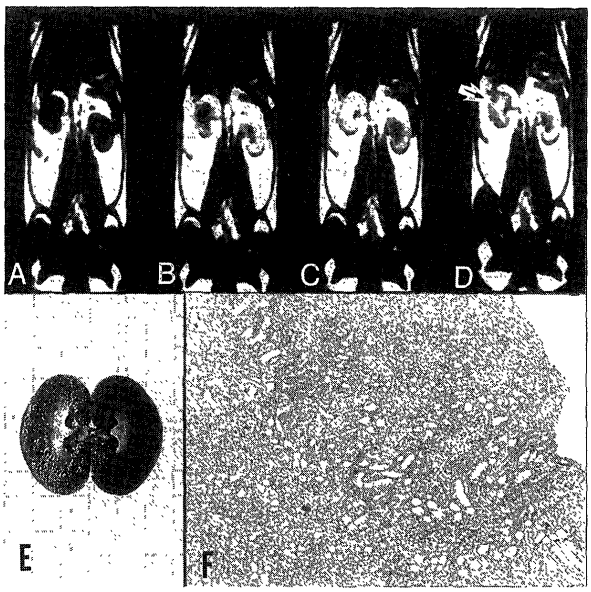

Fig. 4. Dorsal-plane T1-weighted image (Spin echo, TR/TE=200/20 msec) of hydronephrosis (right side in A-D) and normal kidney (left side in A-D). (A: Pre-contrast image. B: Image immediately after injection of gadodiamide. C: 5 min after injection. D: 20 min after injection. E: Gross sagittal appearance. F: Photomicrograph, H.E. stain, × 40). In the pre-contrast image, the hydronephrotic kidney is larger than the normal kidney. Just after administration of gadodiamide injection, signal intensity increased in both cortices, and the band of enhancement gradually moved from the cortex to the medulla in the normal kidney, but no enhancement can be seen in the hydronephrotic medulla. The arrow shows the enhanced pelvis in the normal kidney.

the histological examination, an area of necrosis with gliosis and vacuolation was observed. An ischemic reaction was consistently observed in the entire lesion.

Hepatocellular carcinoma: In the pre-contrast images, the lesion could not be detected in all the rats (n=6) (Fig. 3). Immediately after administration of the contrast agent, markedly enhanced areas were seen in the liver. The gloss findings, various sizes of neoplastic nodules in the liver were noted. Histologically, moderately well differentiated proliferating hepatocytes and trabecular pattern formations were observed, demonstrating hepatocellular carcinoma.

Hydronephrosis: There was a clear difference in signal enhancement between a normal kidney (Fig. 4, left side in A-D) and the hydronephrotic kidney (Fig. 4, right side in A-D). In the pre-contrast image (Fig. 4A), the hydronephrotic kidney was larger than normal. Immediately after administration of the gadodiamide injection, the signal intensity increased in the cortices of both kidneys (Fig. 4B), and the band of enhancement gradually moved from the cortex to the medulla in the normal kidney, but there was no enhancement in the hydronephrotic medulla (Fig. 4C, D). The gross findings revealed dilation of the calix (Fig. 4E). Histologically, pelvic, cortical and medullary tubular dilation were observed and obstructive hydronephrosis was confirmed (n=6) (Fig. 4F).

DISCUSSION

We investigated the diagnostic potential of contrast-enhanced MRI on four experimental disease models of rats, in which MRI without contrast agents may not clearly visualize the lesions. The signal intensity of the respective lesions increased in all the models after the administration of the gadodiamide injection.

In SHRSP, the enhanced area, not delineated in the pre-contrast image, is a relatively new lesion which is due to disruption of the blood brain barrier (BBB) by a stroke. This permits the transfer of the contrast agent into the cerebral tissue [21, 26]. Thus, the gadodiamide injection was considered to shorten the relaxation time of the stroke lesion, and consequently to enhance it. The areas with low-signal-intensity in contrast-enhanced MRI were thought to be old lesions with no blood flows. These results may suggest that contrast-enhanced MRI should be used in diagnosing strokes.

In the MCA occlusion models, the lesion was enhanced in the post-contrast images. This enhancement is also a result of BBB disruption, causing a shortened relaxation time, and is therefore an indication of the degree of damage to the tissue [6, 15].

In hepatocellular carcinoma, markedly enhanced areas were seen in the liver immediately after administration of gadodiamide injection. The contrast effects of gadodiamide injection in rabbit hepatic VX2 tumor models, a model of a metastatic hepatic tumor, were the same as those of meglumine gadopentetate, and showed negative enhancement as we previously reported [35]. The primary

tumor model in this study did however show a positive enhancement, because the blood supply of the primary tumor is derived from the hepatic artery [5, 8, 13, 18, 23]. Most liver tissues receive blood from the portal vein, and there is a time-phase difference between the blood flows in the hepatic artery and the portal vein, thus a very fast scan (25 sec) is of great importance in the diagnosis of liver cancer.

In the normal kidney, the contrast agent was transported quickly (in about 20 min) from the cortex to the medulla, but in hydronephrosis, the signal intensity of the urine within the renal pelvis did not increase. The MR images show the accumulation of gadodiamide in the kidney and its concentration in the urine before excretion. It is suggested that contrast-enhanced MRI can be used to evaluate renal function in a similar way to a creatinine clearance examination, since it provides functional information as well as anatomical information [1–4, 11, 24, 28]. The signal intensity of MR images can be changed by the concentration of the contrast agent. A low dose (0.05 mmol/kg as gadodiamide) gadodiamide injection was therefore used in the hydronephrosis experiment, because there is evidence that the contrast agent penetrates into the renal medulla during normal functions thereby decreasing signal intensity [11, 24]

After an intravenous injection, gadodiamide is distributed in the extracellular space and tends to accumulate in tissues with a rich vasculature [14]. The contrast effects in SHRSP and rats with MCA occlusion are related to differences in capillary permeability, those in rats with hepatocellular carcinoma depend on differences in vascularity, and those in hydronephrotic rats, on vascularity and permeability. Contrast-enhanced MRI has, therefore, the advantage of demonstrating qualitative differences [20, 28].

During these procedures, no significant side effects of the imaging studies were observed. The median lethal dose (LD_{50}) of gadodiamide injection was reported to be approximately 30 mmol/kg in mice, which is much higher than that of others [7, 14, 22, 31].

These results demonstrate the advantages of contrast-enhanced MRI as a new and safe method for the diagnosis of various diseases including tumors and for the monitoring of responses to therapy.

ACKNOWLEDGEMENTS. The authors wish to thank Mr. Yasuhiro Ueshima, Research and Development Department, Siemens-Asahi Medical Systems Ltd., Tokyo, for his useful support and advice in regard to the manipulation of a 2.0 T MRI unit.

REFERENCES

1. Brash, R. C., Weinmann, H. J., and Wesbey, G. E. 1984. Contrast-enhanced NMR imaging: animal studies using gadolinium-DTPA complex. *Am. J. Radiol.* 142: 625–630.
2. Carvin, M. J., Arger, P. H., Kundel, H. L., Axel, L., Dougherty, L., Kassab, E. A., and Moore, B. 1987. Acute tubular necrosis: use of gadolinium-DTPA and fast MR imaging to evaluate renal function in the rabbit. *J. Comput. Assist. Tomogr.* 11: 488–495.
3. Chin, J. L., Stiller, C. R., and Karlik, S. J. 1986. Nuclear magnetic resonance assessment of renal perfusion and preservation for transplantation. *J. Urol.* 136: 1351–1355.
4. Egashira, K., Nakata, H., Sato, N., Nakamura, K., Sugisita, A., and Okamura, T. 1990. Gd-DTPA dynamic MRI of kidney. *J. JMR.* 9: 281–289 (in Japanese with English abstract).
5. Ferrucci, J. T. 1986. MR imaging of the liver. *Am. J. Radiol.* 147: 1103–1116.
6. Grossman, R. I., Joseph, P. M., Wolf, G., Wolf, G., Biery, D., McGrath, J., Kundel, H. L., Fishman, J. E., Zimmerman, R. A., Goldberg, H., and Bilaniuk, L. T. 1985. Experimental intracranial septic infarction: Magnetic resonance enhancement. *Radiology* 155: 649–653.
7. Harpur, E. S., Worah, D., Hals, P., Holtz, E., Furuhama, K., and Nomura, H. 1993. Preclinical safety assessment and pharmacokinetics of gadodiamide injection, a new magnetic resonance imaging contrast agent. *Invest. Radiol.* 28: 28–43.
8. Kadoya, M., Matsui, O., Takashima, T., and Nonomura, A. 1992. Hepatocellular carcinoma: correlation of MR imaging and histopathologic findings. *Radiology* 183: 819–825.
9. Kraft, S. L., Gavin, P. R., Wendling, L. R., and Reddy, V. K. 1989. Canine brain anatomy of magnetic resonance images. *Vet. Radiol.* 30: 147–158.
10. Kuwabara, M., Asanuma, T., Inanami, O., Jin, T., Shimokawa, S., Kasai, N., Kator, K., and Sato, F. 1994. Magnetic resonance imaging of young and aged rat brains under a magnetic field of 7.5 T. *J. Vet. Med. Sci.* 55: 933–938.
11. Leung, A. W. L., Bydder, G. M., Steiner, R. E., Bryant, D. J., and Young, O. R. 1984. Magnetic resonance imaging of the kidneys. *Am. J. Radiol.* 143: 1215–1227.
12. Low, R. N., Francis, I. R., Sigeti, J. S., and Foo, T. K. F. 1993. Abdominal MR imaging: comparison of T2-weighted fast and conventional spin-echo, and contrast-enhanced fast multiplanar spoiled gradient-recalled imaging. *Radiology* 186: 803–811.
13. Mahfouz, A. E., Hamm, B., Taupitz, M., and Wolf, K. J. 1993. Hypervascular liver lesions: differentiation of focal nodular hyperplasia from malignant tumors with dynamic Gadolinium-enhanced MR imaging. *Radiology* 186: 133–138.
14. Masui, T., Saeed, M., Wendland, M. F., and Higgins, C. B. 1991. Occlusive and reperfused myocardial infarcts: MR imaging differentiation with nonionic Gd-DTPA-BMA. *Radiology* 181: 77–83.
15. McNamara, M. T., Brant-Zawadzki, M., Berry, I., Pereira, B., Weinstein, P., Derugin, N., Moore, S., Kucharczyk W., and Brash, R. 1986. Acute experimental cerebral ischemia: MR enhancement using Gd-DTPA. *Radiology* 158: 701–705.
16. Moore, M. P., Gavin, P. R., Kraft, S. L., DeHaan, C. E., Leathers, C. W., and Dorn III, R. V. 1991. MR, CT and clinical features from four dogs with nasal tumors involving the rostral cerebrum. *Vet. Radiol.* 32: 19–25.
17. Morozumi, M., Sasaki, N., Oyama, Y., Uetsuka, K., Nakayama, H., and Goto, N. 1993. Computed tomography and magnetic resonance findings of meningeal syndrome in a leukemic cat. *J. Vet. Med. Sci.* 55: 1035–1037.
18. Nelson, R. C., Umpierrez, M. E., Chezmar, J. L., and Bernardino, M. E. 1988. Delayed magnetic resonance hepatic imaging with gadolinium-DTPA. *Invest. Radiol.* 23: 509–511.
19. Ohashi, F., Kotani, T., Onishi, T., Katamoto, H., Nakata, E., and Fritz-Zieroth, B. 1993. Magnetic resonance imaging in a dog with choroid plexus carcinoma. *J. Vet. Med. Sci.* 55: 875–876.

20. Revel, D., Brasch, R. C., Paajanen, H., Rosenau, W., Grodd, W., Engelstad, B., Fox, P., and Winkelhake, J. 1986. Gd-DTPA contrast enhancement and tissue differentiation in MR imaging of experimental breast carcinoma. *Radiology* 158: 319–323.
21. Runge, V. M., Price, A. C., Wehr, C. J., Atkinson, J. B., and Tweedle, M. F. 1985. Contrast enhanced MRI; Evaluation of a canine model of osmotic blood-brain barrier disruption. *Invest. Radiol.* 20: 830–844.
22. Saeed, M., Wendland, M. F., Takehara, Y., Masui, T., and Higgins, C. B. 1992. Reperfusion and irreversible myocardial injury: Identification with a nonionic MR imaging contrast medium. *Radiology* 182: 675–683.
23. Saini, S., Stark, D. D., Brady, T. J., Wittenberg, J., and Ferrucci, J. T. Jr. 1986. Dynamic spin-echo MRI of liver cancer using gadolinium-DTPA: animal investigation. *Am. J. Radiol.* 147: 357–362.
24. Semelka, R. C., Hricak, H., Tomei, E., Floth, A., and Stoller, M. 1990. Obstructive nephropathy: evaluation with dynamic Gd-DTPA-enhanced MR imaging. *Radiology* 175: 797–803.
25. Stark, D. D., Hendrick, R. E., Hahn, P. F., and Ferrucci, J. T. Jr. 1987. Motion artifact reduction with fast spin-echo imaging. *Radiology* 164: 183–191.
26. Takahashi, M., Fritz-Zieroth, B., Yamaguchi, M., Ogawa, H., Tanaka, T., Sasagawa, S., Chikugo, T., Ohta, Y., and Okamoto, K. 1992. MR imaging of cerebral lesions accompanying stroke in stroke-prone spontaneously hypertensive rats. *Folia Pharmacol. japon* 100: 21–28 (in Japanese with English abstract).
27. Tamura, A., Gotoh, O., and Sano, K. 1986. Focal cerebral infarction in the rat: 1. operative technique and physiological monitorings for chronic model. *Brain and Nerve* 38: 747–751 (in Japanese with English abstract).
28. Tateno, Y. and Yamada, K. 1993. The Atlas of MRI and CT in Cats and Dogs. University of Tokyo Press, Tokyo.
29. van Bree, H., Degryse, H., Van Ryssen, B., Ramon, F., and Desmidt, M., 1993. Pathologic correlations with magnetic resonance images of osteochondrosis lesions in canine shoulders. *J. Am. Vet. Med. Assoc.* 202: 1099–1105.
30. van Bree, H., Van Ryssen, B., Degryse, H., and Ramon, F. 1995. Magnetic resonance arthrography of the scapulohumeral joint in dogs, using gadopentetate dimeglumine. *Am. J. Vet. Res.* 56: 286–288.
31. Vogl, J. T., Mack, G. M., Juergens, M., Bergman, C., Grevers, G., Jacobsen, F. T., Lissner, L., and Felix, R. 1993. Skull base tumors: Gadodiamide injection-enhanced MR imaging-drop-out effect in the early enhancement pattern of paragangliomas versus different tumors. *Radiology* 188: 339–346.
32. Weisburger, J. H., Madison, R. M., Ward, J. M., Viguera, C., and Weisburger, E. K. 1975. Modification of diethylnitrosamine liver carcinogenesis with phenobarbital but not with immunosuppression. *J. Natl. Cancer Inst.* 54: 1185–1188.
33. Whelan, H. T., Clanton, L. A., Moore, P. M., Tolner, D. J., Kessler, R. M., and Whetsell, W.O. Jr. 1987. Magnetic resonance brain tumor imaging in canine glioma. *Neurology* 37: 1235–1239.
34. Wolf, R. F. E., Lam, K. H., Mooyaart, E. L., Bleichrodt, R. P., Nieuwenhuis, P., and Schakenrad, J. M. 1992. Magnetic resonance imaging using a clinical whole body system: an introduction to a useful technique in small animal experiments. *Lab. Anim.* 26: 222–227.
35. Yamada, K., Kato, H., Jinbo, T., Sugihara, H., Nakashima, K., Koga, M., Shishido, F., Tateno, Y., and Ikehira, H. 1993. MR imaging of experimental hepatic metastasis in the rabbit contrast enhancement effect of DV-7572 injection. *Jpn. Pharmacol. Ther.* 21: 5–15 (in Japanese with English abstract).
36. Yamada, K., Miyahara, K., Sato, M., Hirose, T., Yasugi, Y., Matsuda, Y., and Furuhama, K. 1995. Magnetic resonance imaging of the central nervous system in the kitten. *J. Vet. Med. Sci.* 57: 155–156.
37. Yamada, K., Miyahara, K., Sato, M., Hirose, T., Yasugi, Y., Matsuda, Y., and Furuhama, K. 1995. Optimizing technical conditions for magnetic resonance imaging of the rat brain and abdomen in a low magnetic field. *Vet. Radiol. Ultrasound.* 36: 523–527.